Acta Montanistica Slovaca
ISSN 1335-1788
actamont.tuke.sk

Monitoring and modelling the deformation state of a dyke of a flotation tailings reservoir of a copper ore mine

Zygmunt NIEDOJADŁO[1], Tomasz STOCH[2], Janusz JURA[3], Paweł SOPATA[4], Artur WÓJCIK[5] and Dawid MROCHEŃ[6]*

Authors' affiliations and addresses:
[1] AGH University of Science and Technology, Faculty of Mining Surveying and Environmental Engineering, Mickiewicza av. 30, Cracow, Poland
e-mail: niedojad@agh.edu.pl

[2] AGH University of Science and Technology, Faculty of Mining Surveying and Environmental Engineering, Mickiewicza av. 30, Cracow, Poland
e-mail: tomst@agh.edu.pl

[3] AGH University of Science and Technology, Faculty of Mining Surveying and Environmental Engineering, Mickiewicza av. 30, Cracow, Poland
e-mail: jura@agh.edu.pl

[4] AGH University of Science and Technology, Faculty of Mining Surveying and Environmental Engineering, Mickiewicza av. 30, Cracow, Poland
e-mail: Pawel.Sopata@agh.edu.pl

[5] AGH University of Science and Technology, Faculty of Mining Surveying and Environmental Engineering, Mickiewicza av. 30, Cracow, Poland
e-mail: awoj@agh.edu.pl

[6] Strata Mechanics Research Institute, Polish Academy of Sciences, Reymonta 27, 30-059, Cracow, Poland
e-mail: dawid.mrochen@imgpan.pl

***Correspondence:**
Tomasz Stoch, AGH University of Science and Technology, Faculty of Mining Surveying and Environmental Engineering, Mickiewicza av. 30, Cracow, Poland
tel.: +48126172262
e-mail: tomst@agh.edu.pl

How to cite this article:
Niedojadło, Z., Stoch, T., Jura, J., Sopata, P., Wójcik, A. and Dawi Mrocheń, D. *(2023).* Monitoring and modelling the deformation state of a dyke of a flotation tailings reservoir of a copper ore mine. *Acta Montanistica Slovaca*, Volume 28 (1), 123-140

DOI:
https://doi.org/10.46544/AMS.v28i1.11

Abstract
The mining areas of the copper ore mines in Poland contain tailings storage facilities. Because of operational safety issues and to minimize the exposure of local neighbourhoods to the risk of such reservoirs failing, mining operations are limited during the period of waste storage, thereby reducing the impact of exploitation on these objects. Nevertheless, continuous monitoring and analysis of the deformation state of reservoirs and associated facilities are required. Monitoring is most often carried out using geodetic methods, while the deformation analysis is based on determining the displacements of control points and making short- and long-term forecasts of changes in land surface deformation.
Presented here is an analysis of changes in the state of displacements and dyke deformations of a currently closed copper flotation tailings reservoir that was used in the 1970s. After the storage of waste was stopped, an intensive two-stage mining operation was carried out under the reservoir. The results obtained from the geodetic monitoring of displacements and deformations of the reservoir dyke are compared with the model values, and the usefulness of the applied theoretical model for describing the vertical and horizontal displacements and horizontal deformations is verified. Based on the comparison results, a hypothesis is presented regarding the causes of the actual condition of the movements of the reservoir dam crest against the background of the expected movements obtained from theoretical modelling. The presented conclusions revise a very rigorous approach to protecting flotation tailings reservoirs against the effects of underground mining.

Keywords
forecasting of land surface deformation, mining subsidence, horizontal displacements, Knothe model, tailing storage facilities

Introduction

In recent years, experts have faced increasing difficulties in forecasting how underground mining impacts the land surface, these difficulties being related to the concentration of extraction, changing mining and geological conditions, and having to account for old mining works. The analysis of the impact of exploitation covers existing facilities and those planned for future implementation (Kwiatek, 2007). This applies to objects located both on the surface and inside the rock mass (mining shafts) (Kwinta, 2012a), and deformation forecasting refers increasingly to momentary and extreme states (values) in time.

Special objects in mining areas are flotation tailings reservoirs, whose function and size mean that they are under special supervision by mining services. The operational safety of this type of facility determines the continuity of a mine's operation, and damage to dams poses a risk of industrial and natural disasters (Owen, Kemp, Lèbre, Svobodova, & Pérez Murillo, 2020). For this reason, such objects are subjected to periodic geodetic observations (Jura, Niedojadło, & Stoch, 2013). In addition to classic surveying techniques such as total-station measurements and precise levelling, methods based on global navigation satellite systems (GNSS) are also used to monitor dams. Observation points located on a dam allow conclusions about its stability. Nowadays, unmanned aerial vehicles (Dawei, Lizhuang, Demin, Baohui, & Lianglin, 2020; Stupar, Rošer, & Vulić, 2020) are being used increasingly to observe mining areas, both to monitor subsidence (Ćwiakała et al., 2020) and to determine horizontal displacements (Puniach, Gruszczyński, Ćwiąkała, & Matwij, 2021). In the case of horizontal displacements, the considerable usefulness of terrestrial laser scanning (Matwij, Gruszczyński, Puniach, & Ćwiąkała, 2021) for urbanized areas has also been demonstrated. To monitor reservoir dams, satellite radar interferometry (interferometric synthetic aperture radar) is also used (Gama, Paradella, Mura, & de Oliveira, 2019; Grebby et al., 2021). This method also allows assessment of the impact of mining operations in the vicinity of the reservoir (whether and to what extent they affect the facility), as well as strong mining tremors on the ground surface (A. A. Malinowska, Witkowski, Guzy, & Hejmanowski, 2018; Sopata, Stoch, Wójcik, & Mrocheń, 2020).

The inspiration for addressing the issue of forecasting that accounts for the instantaneous and extreme values of deformation in time was analyzing the impact of a planned mining operation on an existing hydrotechnical facility in the expansion phase. The deformation analysis accounts for safe (currently accepted) values of increments of horizontal strains and slopes that should not endanger the proper functioning of the object. The results of research and analyses conducted in this study answered the question as to whether the accepted permissible deformation values for this type of earth structure are too strict.

This type of analysis is relatively difficult and requires correct modelling of the deformation phenomenon in the long term. Among other aspects, it is important to establish correct parameters of the calculation model corresponding to the local geological and mining conditions (Kowalski, 2007, 2011; Kwinta, 2012b). The models used in Poland and worldwide for forecasting deformation of the ground surface and rock mass are often based on assumptions simplifying the phenomenon of deformation caused by underground mining. Empirical models are used (Jiang, Misa, Tajduś, Sroka, & Jiang, 2020; Tajduś, 2015) as well as geometric-integral models based on various functions of influences (Kratzsch, 1983; Peng, 1992; Reddish & Whittaker, 2012). Also used to forecast the deformation of mining areas are neural networks (Ambrožič & Turk, 2003; Gruszczyński, 2007) and numerical methods, including the finite-element and finite-difference methods (Tajduś, 2009; Xu et al., 2013) and the discrete element method (Fathi Salmi, Nazem, & Karakus, 2017).

The presented analysis of the impact of mining exploitation concerns an inactive mining waste treatment facility. For over 40 years, geodetic observations have been made on the object to determine selected deformation indicators (Jóźwik, Jura, Szymczyk, Mazur, & Tarasek, 2000; Jura, 1994) and assess the stability of the earth structure. The conducted analyses concern one object subjected to the influence of mining exploitation; therefore, they do not constitute a basis for broad generalization. This case, however, provides a general overview of the problem, which may be taken into account in other facilities of this type.

Herein, observed subsidence and horizontal displacement and deformation values are compared with those obtained theoretically based on the Knothe model (Knothe, 1957; Agnieszka Malinowska, Hejmanowski, & Dai, 2020). The Knothe model has been used in mining throughout the world, including in Australia (Byrnes, 2003), China (Yan, Lun, Yue, Preuβe, & Sroka, 2018), the Czech Republic (Jiránková, Waclawik, & Nemcik, 2020), and the USA (Karmis, Agioutantis, & Andrews, 2008). The presented methodology allows assessment of the quality of *a priori* forecasting and *a posteriori* modelling of deformation indicators. Apart from subsidence and horizontal deformations, great emphasis is placed on presenting and analyzing the vectors of horizontal displacement, which are important for analyzing the functional safety of a hydro-technical structure.

On the basis of the obtained results, a number of analyses are carried out. The modelling results for the observed phenomenon are verified as converging with the measurements of the actual state of deformation of the land surface and reservoir dyke due to the exploitation of subsequent mining fields. This allows for conclusions regarding the object in question, and an attempt is made to provide the causes of non-compliance of the model with the observed displacements and deformations.

Material and Methods

Registration of land surface changes using geodetic methods allows for the determination of a number of deformation indicators, the significance of which depends on the object under observation. Apart from basic indicators such as subsidence (s), tilt (T), or horizontal deformation (ε), horizontal displacement (u) also plays an important role, especially in relation to special objects located in the mining area. The importance of this indicator increased with the implementation of Global Positioning System (GPS) technology in deformation research in the early 1990s.

Area of interest

The research area is in the Legnica–Głogów Copper District (LGCD) in southwest Poland, and the analysis covers a flotation tailings reservoir with an area of 5.7 km^2 located in the mining area. It is based on a flat slope of hills in the north and is bounded by an earth dam (dyke) on the south side for a length of 6.76 km. The height of the dyke reaches 22 m, and the width of the embankment is 97 m at the base and 4 m at the crest (Fig. 1). Put into operation in 1968, it was used as an active landfill for flotation tailings until 1980. The deposit exploitation under the reservoir began in the second half of the 1970s, and this has continued with varying intensity to date (Piestrzyński, 2008).

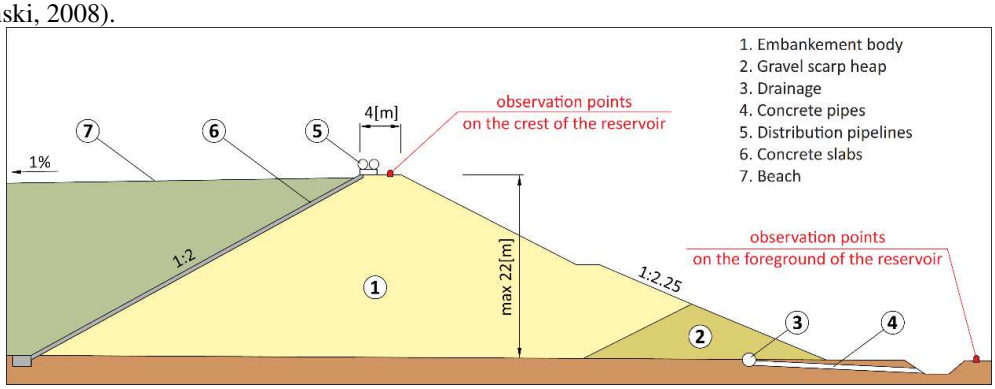

Fig. 1. The cross-sectional structure of dyke (adapted from Piestrzyński, 2008)

Geodetic observations

Observations of the crest of the earth dam were analyzed. The horizontal subsidence and deformations analysis was performed for stabilized points at distances of approximately every 24 m (yellow and black points) and for horizontal displacements every 100 m (yellow points). The results of measurements carried out at points located in the foreground of the dam on the southern side were also partially used (Fig. 2).

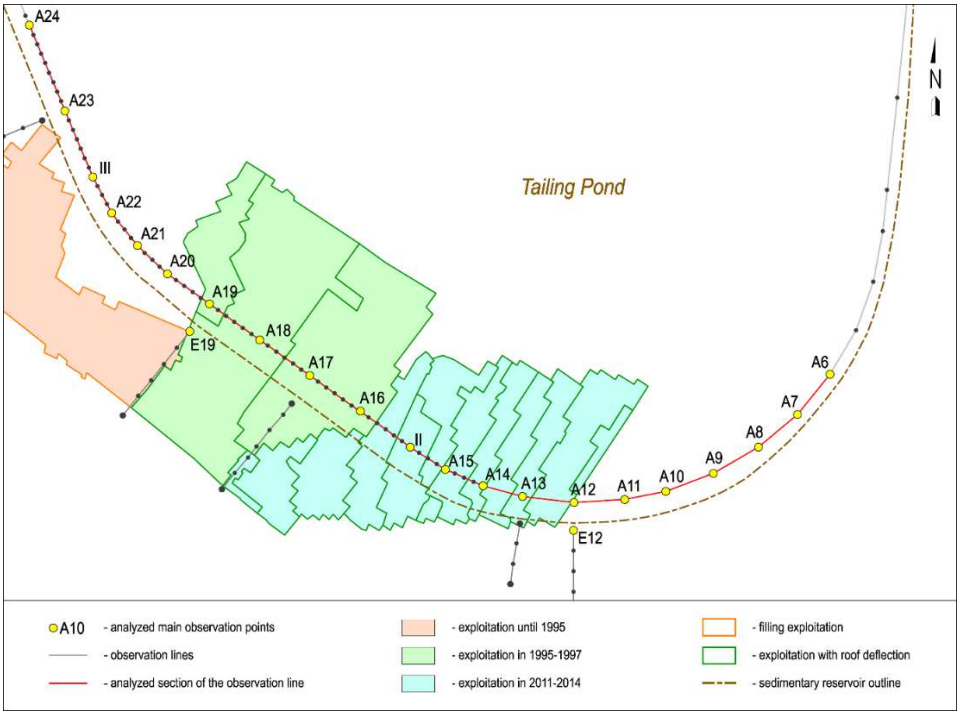

Fig. 2. Scheme of exploitation fields and analyzed observation (calculation) points

The subsidence was analyzed based on the part of the observation line on the crest of the reservoir between points A6 and A23. For the analysis of horizontal displacements, the section between points A8 and A20 was selected, consisting of the main points spaced approximately every 100 m. Measurements of changes in length were made only from point A14 toward the west. For this reason, for the analysis of horizontal deformations, a shorter section of the observation line (A14–A20) was adopted, with intermediate points spaced every 24 m.

The network of observation points (Fig. 2) is subjected to annual control observations, including measuring the current *X*, *Y*, and *H* spatial coordinates (EPSG:2176). The horizontal coordinates of the observation network points have been measured since 1973, and GPS (GNSS) technology has been used since 1994 for tying. The measurements are made using a static method, and the designed measurement cycle, taking into account the terrain conditions and tying method, allows the coordinates of points to be obtained to an accuracy of approximately ±7 mm. Points determined using GNSS technology are tied to traverses measured with a precise total station (Leica TCA2003), thanks to which, in terms of accuracy, a practically homogeneous network is created. Carried out by means of precise geometric levelling (Leica DNA2003 level), the height measurements are currently tied to benchmarks located at the shaft stations of mining shafts. The height of the tie benchmarks on the shaft square is determined for these shaft stations. The observation results make it possible to assess the accuracy of determining the heights of points in successive measurement series to be ±3 mm.

Because of the measurement techniques used, it was assumed that the analyses would be based on data obtained in the years 1994–2019. Such a limitation of the scope of the analyzed data allows for the assumption that the results of the observations no longer show the effects of compaction of the material from which the dam is made (which is also confirmed by geotechnical observations). In addition, the subject of the analysis is uniform observation material obtained using the same class of equipment throughout the analyzed period.

Knothe method

According to the geometric-integral model of Knothe (Knothe, 1957), the distribution of the subsidence of points in the cross-section perpendicular to the rectilinear edge of the mining exploitation front with a half-plane dimension is described by

$$s(x) = -\frac{a \cdot m}{r} \cdot \int_{x}^{+\infty} exp\left(-\pi \frac{\lambda^2}{r^2}\right) d\lambda, \tag{1}$$

where *a* is the exploitation factor and *m* is the thickness of the exploited deposit. The range of exploitation *r* [m] is given by

$$r = \frac{H}{tan\beta}, \tag{2}$$

where *H* is the depth [m] of exploitation and β is the influence-range angle.

Further indicators characterizing the state of deformation are the horizontal deformation ε and the horizontal displacement *u*. The values of the components u_x and u_y of the horizontal displacement (Eq. 3) in the directions of the axes of the adopted coordinate system are proportional to the value of the slope *T* of the subsidence trough profile, i.e., to the first derivative of the subsidence (Eq. 1) in the directions of the axes of the adopted coordinate system:

$$u_x = -B\frac{\partial s}{\partial x}, \qquad u_y = -B\frac{\partial s}{\partial y}, \tag{3}$$

$$u_{max} = \sqrt{u_x^2 + u_y^2}, \tag{4}$$

$$\varepsilon_x = \frac{\partial u_x}{\partial x} = -B \cdot K_x = u_x = -B\frac{\partial s^2}{\partial x^2}, \tag{5}$$

$$\varepsilon_y = \frac{\partial u_y}{\partial y} = -B \cdot K_y = u_y = -B\frac{\partial s^2}{\partial y^2}. \tag{6}$$

where *B* is known as the coefficient of horizontal displacement.

Analyzing the results of measurements from the Upper Silesian Coal Basin (USCB) in Poland, Budryk (Budryk, 1953) determined the value of the coefficient *B* given by Eq. (7) for the terrain surface:

$$B = \frac{r}{\sqrt{2\pi}} = 0.4\, r. \tag{7}$$

Subsequent analyses of the observational material (Popiołek & Ostrowski, 1978) from the areas affected by mining operations in the USCB showed that this value was

$$B = 0.32\, r. \tag{8}$$

In the case of copper ore mines in the LGCD, studies carried out between 1995-1996 (Popiołek, 1995, 1996) showed differentiation of the deformation process in terms of horizontal compressive (Eq. 9) and tensile (Eq. 10) deformations. The following values of the coefficient B were established:

$$B(+) = 0.30\,r, \quad \text{(tension)} \tag{9}$$
$$B(-) = 0.36\,r. \quad \text{(compression)} \tag{10}$$

For the initial analysis of the distribution of the forecast values of deformations and horizontal displacements in the analyzed case, the average value of $B = 0.32\ r$ was adopted according to Equation 8.

The total impact of mining exploitation is revealed on the surface after the exploitation. The equation for the trough profile includes the so-called time function $f_1(t, c)$, whose parameter is the time coefficient c, which characterizes the average speed of the passage of mining influences through the rock mass. Therefore, the equation describing the land surface subsidence can be written as

$$s(x) = \frac{s_{max}}{r^2} \cdot f_1(t,c) \cdot \int_x^{+\infty} exp\left(-\pi \frac{\lambda^2}{r^2}\right) d\lambda, \tag{11}$$

where t is the time from the end of operation and c is the global time factor. In the approach by Knothe (Knothe, 1953), the time function has the form

$$f_1(t,c) = exp(1 - ct). \tag{12}$$

Accounting for the modifications to the model introduced by Sroka and Schober (Sroka & Schober, 1983) and Hejmanowski (Hejmanowski, 2004), the global time factor c for the conditions of copper ore mines in Poland is (Agnieszka Malinowska et al., 2020)

$$c = \frac{\xi \cdot \eta}{\xi + \eta}\ [year^{-1}], \tag{13}$$

where ξ is the relative speed of convergence of the excavated workings, and η is the relative speed of transition of the deformation process in the rock mass.

Results

The analysis covers the impact of exploitations carried out by a chamber-pillar system with hydraulic filling (1994–1995) and with roof deflection in two periods (1995–1997 and 2011–2014). This made it possible to assess the accuracy of forecasting for various operating conditions.

Subsidence

First, the analysis covered the subsidence values of the observation-line points along the section between points A6 and A23 (Fig. 4). This showed that the mining operations resulted in both direct and indirect mining influences. In the period 1995–2019, at some points of the line, subsidence of approximately 150 mm was observed (Fig. 3), which is attributed to only indirect operating impacts. The factor causing these changes was the drainage of the rock mass, which is characteristic of the analyzed area. It triggers the process of continuous drainage of aquifers in the rock mass, which in turn causes the phenomenon of compaction of rock layers observed as large spatial subsidence of the terrain surface (Guzy & Malinowska, 2020; Niedojadło, Sieradzy, & Spólnik, 2012; Witkowski, 2017). Measurements and analyses carried out in this area indicate the occurrence of dehydration subsidence with values ranging from 5 to 10 mm/year. These values are characterized by variable dynamics, depending on the area of the deposit and the stage of exploitation.

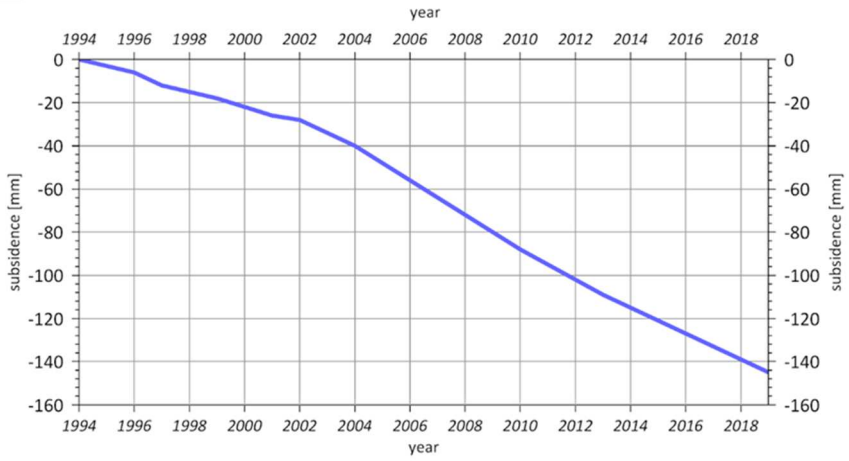

Fig. 3. Subsidence caused by rock-mass dehydration

Because of the large-scale nature of the phenomenon, it was assumed that in the analyzed period (1995–2019), the subsidence of all points of the observation-line section was burdened with the same effect of drainage of aquifers. Therefore, the annual subsidence of all points was reduced by the value of dehydration subsidence. The values of subsidence corrected in this way represent only the effects of mining (Fig. 4).

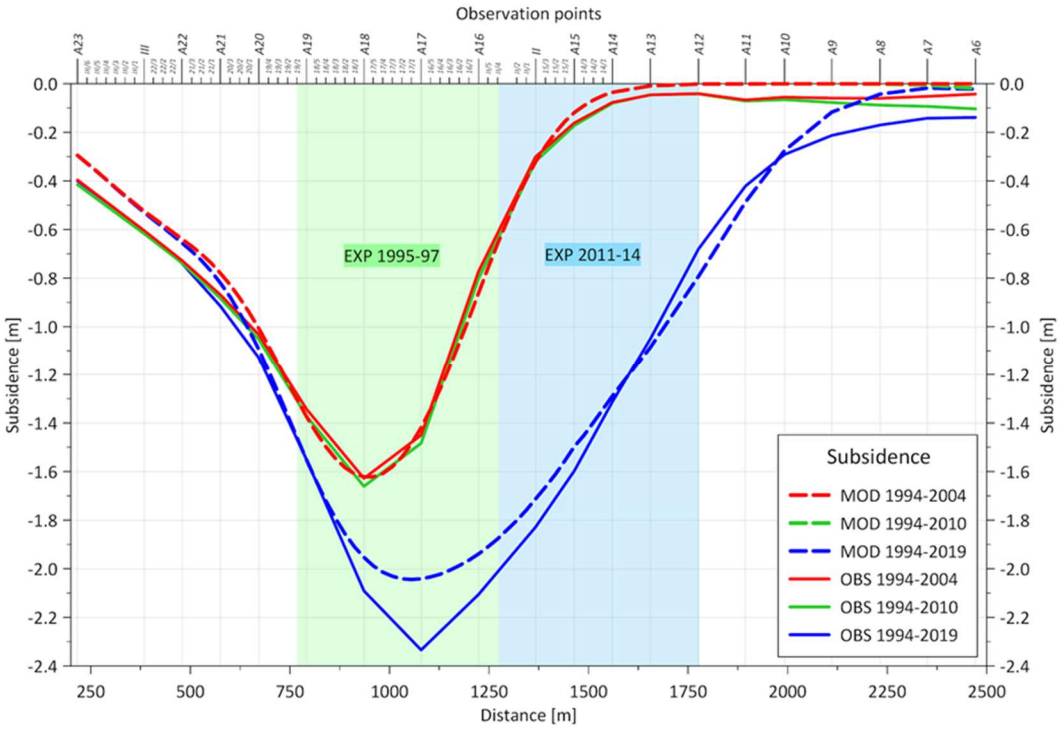

Fig. 4. Reduced subsidence in 1994–2004, 1994–2010, and 1994–2019 along analyzed line

The distribution of measured subsidence (Fig. 4) was the basis for verifying the basic parameters of the Knothe model. The *a posteriori* values of the parameters based on measuring the subsidence are $\tan\beta = 1.8$ and $a = 0.52$. The parameters were determined using the least-squares method (Gruszczyński, Niedojadło, & Mrocheń, 2018; Kwinta, 2011; Witkowski, 2014) and do not differ significantly from the standard values adopted for mining with roof deflection in the conditions of the analyzed copper ore mine ($\tan\beta = 1.7$ and $a = 0.50$).

The correctness of the parameterization of the calculation model is evidenced by the obtained convergence of the measured subsidence reduced by the values of the dehydration subsidence (Fig. 4, solid lines) and the modelled subsidence (Fig. 4, dashed lines). The lack of increments in the subsidence between 2004 and 2010 (red and green solid lines) means that by 2004 the effects of the mining operation carried out in 1995–1997 (green area in Fig. 4) were fully revealed. The maximum subsidence after the exploitation in 1995–1997 was $s_{obs} \approx 1.6$ m on the dyke, and it increased after the second stage of exploitation in 2011–2014 (blue area in Fig. 4) to $s_{obs} \approx 2.3$ m (theoretical value: $s_{mod} \approx 2.1$ m).

Time factor

The standard parameter values (set A) for the calculation model used in the LGCD are

$$\xi = 0.52\ year^{-1};\ \eta = 3.0\ year^{-1} \rightarrow c = 0.44\ year^{-1},$$

for which the distributions of the measured and modeled subsidence values are currently not consistent. Therefore, in the calculations of the dynamic deformation indexes, the following parameter values were adopted (set C):

$$\xi = 3.0\ year^{-1};\ \eta = 6.0\ year^{-1} \rightarrow c = 2.0\ year^{-1},$$

for which the best compliance of the distribution of the subsidence was obtained in the period 1994–2019. The correctness of the adopted parameters is confirmed by the high convergence of the distribution of the modelled and observed subsidence presented in Fig. 5.

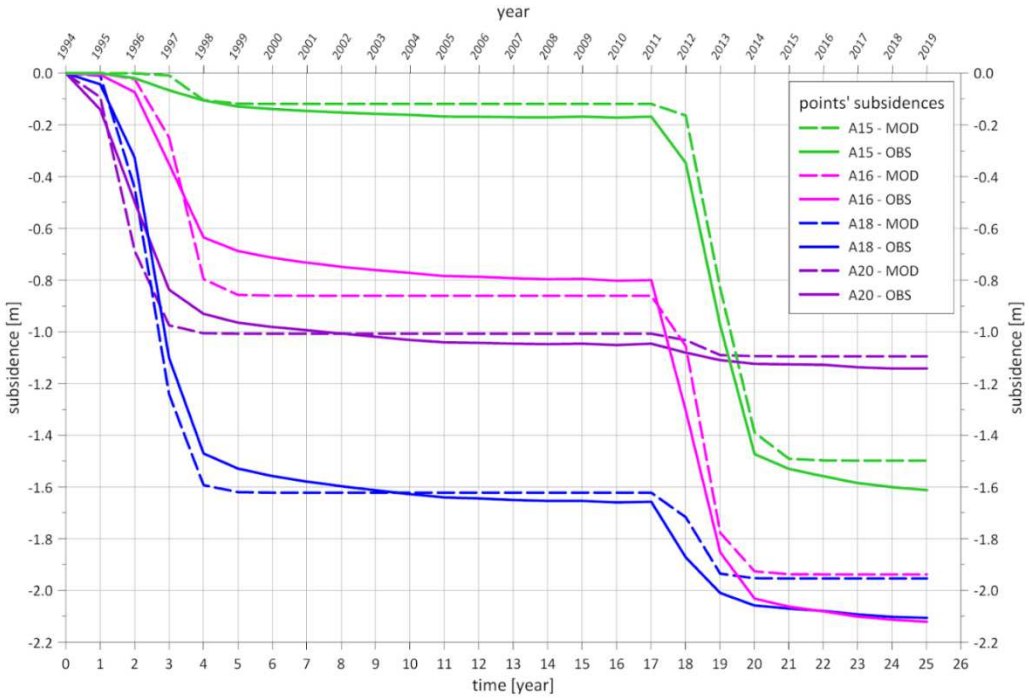

Fig. 5. Subsidence of analyzed points A15, A16, A18, and A20 in 1994–2019

In three years (1995–1998), the maximum increase in subsidence for point A18 (Fig. 5, blue lines) was $\Delta s_{obs} \approx 1.43$ m and $\Delta s_{mod} \approx 1.54$ m, which means a monthly increase of approximately 4 cm/month.

In the second stage of exploitation (2011–2014), the highest increase in subsidence in only two years (2012–2014) was for point A15 (Fig. 5, green lines), i.e., $\Delta s_{obs} \approx 1.06$ m and $\Delta s_{mod} \approx 1.10$ m, which corresponds to a monthly increase of subsidence of approximately 4.5 cm/month. Therefore, we observe a shorter period of maximum increases in subsidence and an increase in the dynamics of the phenomenon.

The subsidence for point A16, located closest to the eastern edge of the field exploited in 1995–1997 (Fig. 2), was analyzed in detail. Calculations of subsidence changes at the point in 1994–2011 were performed for three sets of parameters on the basis of the works by Niedojadło (Niedojadło, 2008):

$$\text{set A: } \xi = 0.52\ year^{-1};\ \eta = 3.0\ year^{-1} \rightarrow c = 0.44\ year^{-1}\ \text{(standard parameters)},$$
$$\text{set B: } \xi = 1.00\ year^{-1};\ \eta = 3.0\ year^{-1} \rightarrow c = 0.75\ year^{-1},$$
$$\text{set C: } \xi = 3.00\ year^{-1};\ \eta = 6.0\ year^{-1} \rightarrow c = 2.00\ year^{-1}\ \text{(optimal parameters)}.$$

The distributions of the observed and modelled values of the subsidence of point A16 for the adopted sets of model parameters are presented in Fig. 6.

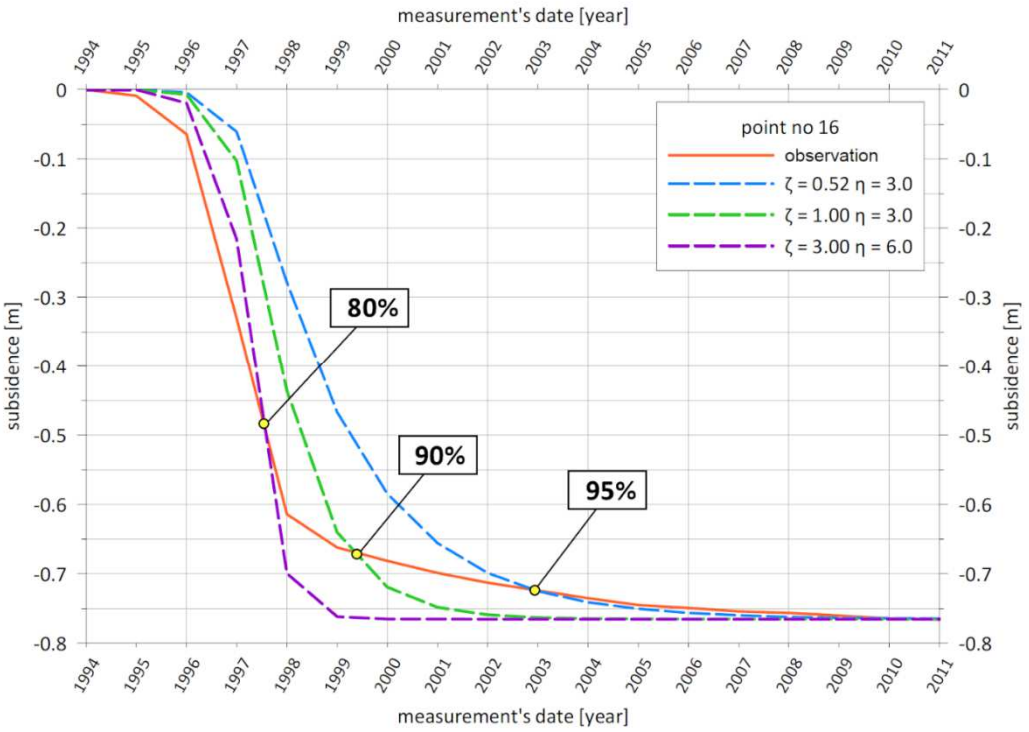

Fig. 6. Dynamic values of observed and modelled subsidence

From analyzing the graph in Fig. 6, the following can be concluded.

Assuming standard parameters (set A), the main phase of the subsidence is described incorrectly. The theoretical values are consistent with the measured values in only the final phase of the phenomenon, in which approximately 95% of the total subsidence (2003) is found.

For parameter set B, a convergence of the modelled subsidence with those measured at the moment of reaching approximately 90% of the final values of vertical displacements (in 1999–2000) can be observed.

For parameter set C, the starting (1996) and ending (1997) times of the main incremental phase of the deformation indexes are determined correctly until approximately 80% of the final values are reached. The termination of disclosure of total influences is modelled too early (1999). However, with this set of parameters, the most important phase of exploitation impact and the disclosure of the maximum values of the deformation indicators are described quite correctly.

Therefore, for the assumed theoretical function (11), it is not possible to correctly describe the actual course of the dynamics of the phenomenon, assuming specific parameter values for the entire analyzed period.

Horizontal displacement

The horizontal displacement u is an important indicator of the deformation of the analyzed object, showing the general tendency of the ground on which the dyke and the reservoir are placed. Locally increased values of horizontal displacement may signal a greater threat to the safety of the reservoir than those of horizontal deformation (ε). The least-favourable situation is when the local displacement vectors have increased values and are perpendicular to the axis of the dyke. However, despite the great importance of horizontal displacement in the safety assessment of the dykes of sedimentary ponds, it is yet to be accounted for.

The possibility of determining horizontal displacements appeared only in the 1990s thanks to GNSS technology; such measurements were impossible in the 1970s and 1980s. Nowadays, GNSS technology is used widely, mainly because of its accuracy. Thanks to this measurement technology, it is possible to perform a detailed analysis of the displacements of points on the ground surface, which allows for the verification of existing views on the horizontal movements caused by underground mining. The case presented herein shows the distribution of horizontal displacements of the terrain surface deviating from those presented in most mining impact models (Stoch, 2019; Tajduś, 2015).

Figure 7 shows the distribution of the maximum asymptotic values of horizontal displacement along the observation line for three periods: (i) after the operation in 1995–1997, (ii) after the operation in 2011–2014 (increase in the value of displacement), and (iii) the total values (1995–2019). The characteristic maximum values are presented in Table 1.

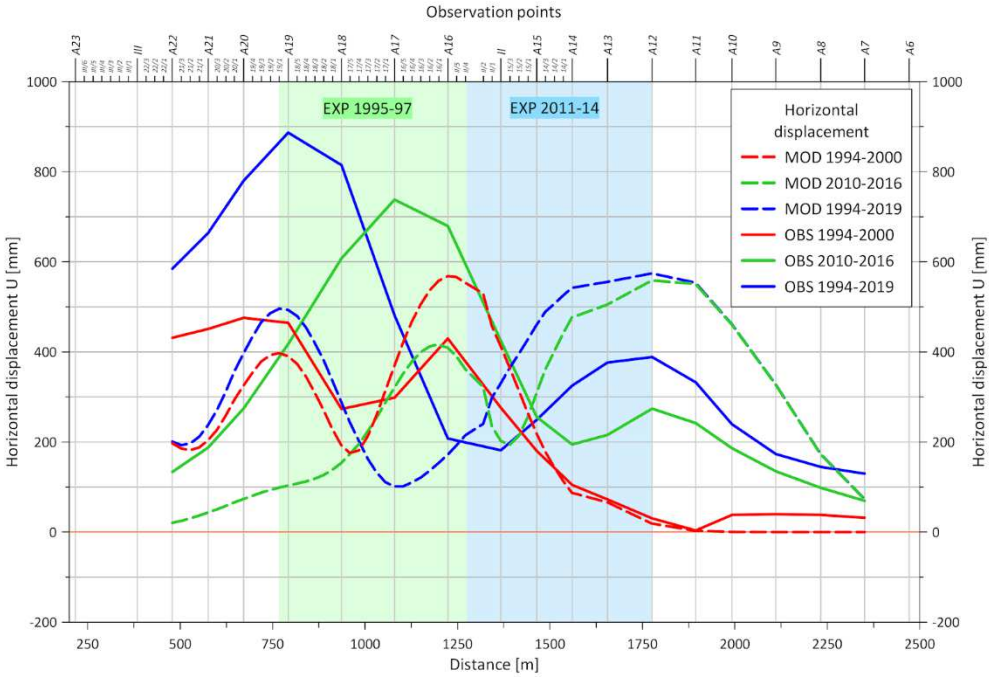

Fig. 7. *Distribution of maximum displacement values (u_{max}) at observation-line points*

Tab. 1. Maximum horizontal displacement u_{max} [m] over different year ranges

1994–2000				2010–2019				1994–2019			
No.	Observed	Modelled	Difference	No.	Observed	Modelled	Difference	No.	Observed	Modelled	Difference
A19	0.48	0.41	0.07	A17	0.73	0.42	0.31	A19	0.89	0.51	0.38
A16	0.43	0.56	-0.13	A12	0.27	0.56	-0.29	A12	0.41	0.57	-0.16

Horizontal deformation

Length changes, and therefore also horizontal deformations, were determined on the analyzed dyke only from point A14. Therefore, it is impossible to compare the deformations observed and modelled in the area of the eastern border of the analyzed fields exploited in 1994–2014.

Their values for individual sides were determined from the difference of the modelled horizontal displacements at the endpoints of the sides (Eq. 13) calculated in the direction of the observation-line segment (Stoch, 2019):

$$\varepsilon_{i,i+1} = \frac{\Delta u_{i,i+1}}{d_{i,i+1}} = \frac{u_{i+1} - u_i}{d_{i,i+1}}, \tag{13}$$

where $\varepsilon_{i,i+1}$– [mm/m] is the horizontal deformation of the measuring section between points i and i+1, u_i, u_{i+1}– [mm] are the modelled horizontal displacements of the endpoints of the observation-line segment $(i, i+1)$ toward this segment, and $d_{i,i+1}$ [m] is the length of the observation-line segment.

This is consistent with the methodology of determining the actual observed deformation values as a relative change in the length of the measuring section (Ostrowski, 2015):

$$\varepsilon_{i,i+1} = \frac{\Delta d_{i,i+1}}{d_{i,i+1}}, \tag{14}$$

where $\varepsilon_{i,i+1}$– [mm/m] is the horizontal deformation of the measuring section between points i and i+1, $\Delta d_{i,i+1}$– [mm] is the observed change in the length of the measurement segment of the observation line $(i, i+1)$ in two different series of observations, and $d_{i,i+1}$– [m] is the length of the observation-line segment.

In principle, the modelled and measured deformation values should be compared in accordance with this calculation method. Also, note that the differences are small when comparing the deformations modelled with both methods.

Figure 8 shows the distributions of the theoretical deformation values at the measurement points according to Eqs. (5) and (6), as proportional to the second derivative of the subsidence, with the proportionality coefficient according to Eq. (8). Figure 9 shows the theoretical values of horizontal deformations determined on the measuring sections for which periodic changes in length were found, and Table 2 summarizes the maximum values of horizontal deformations for the subsequent stages of the analyzed operation.

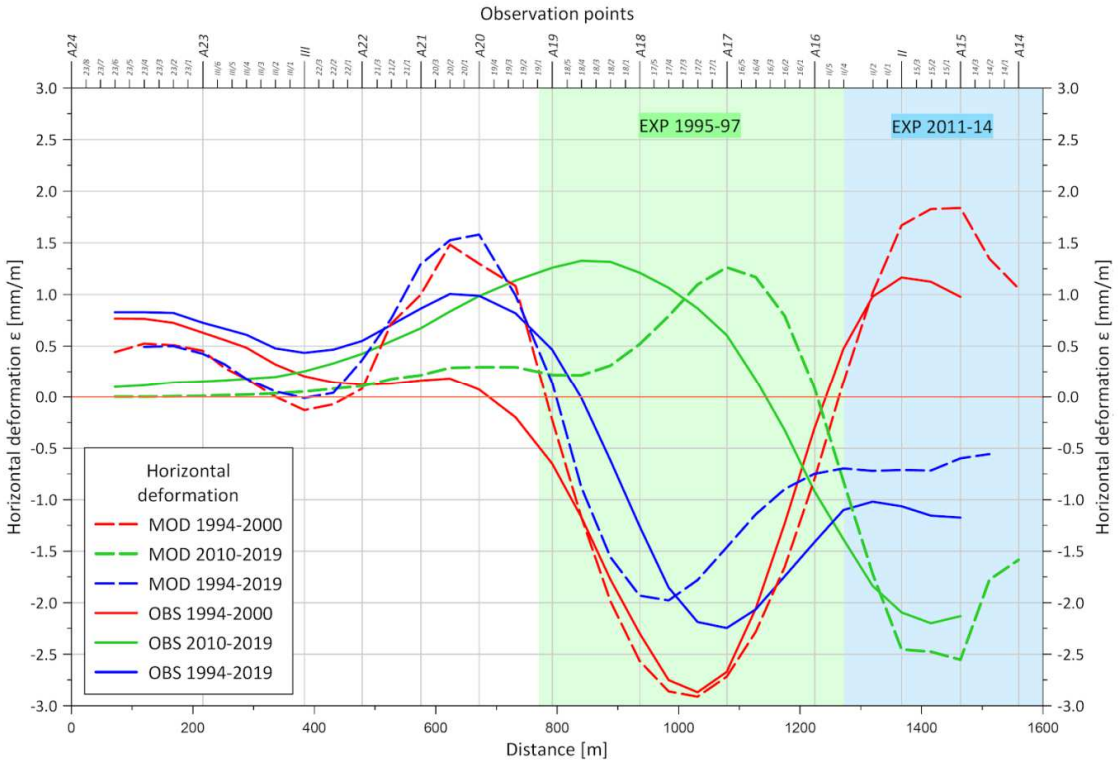

Fig. 8. Comparison of observed horizontal deformations of sections of observation line and those modelled at points

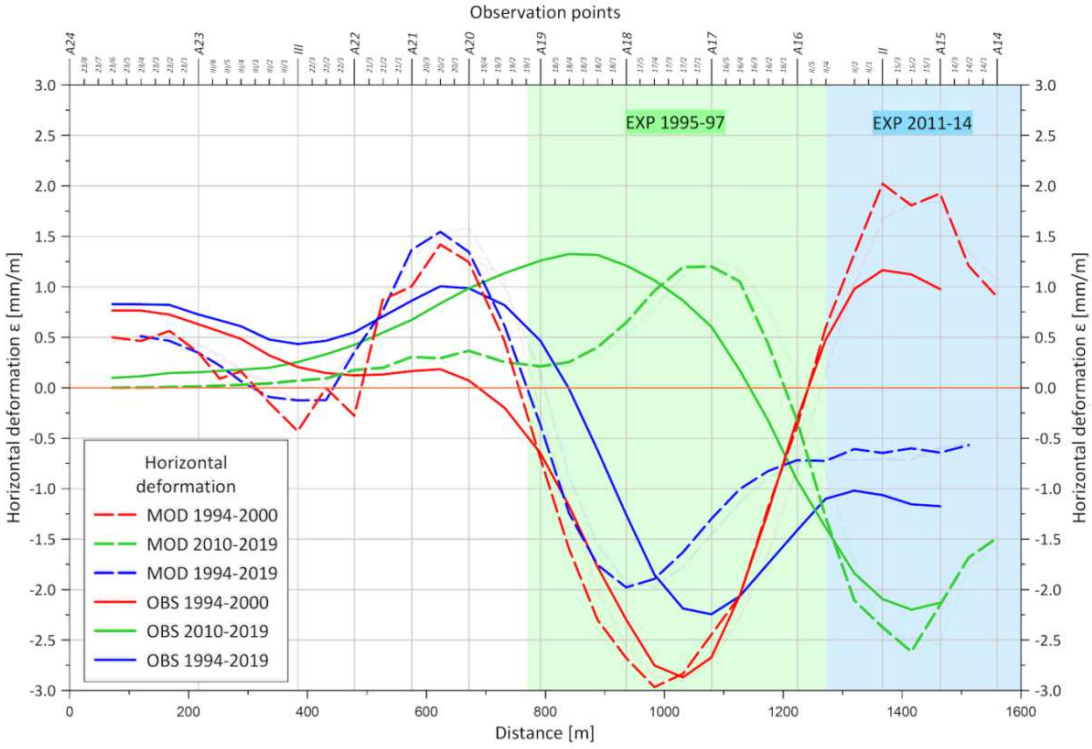

Fig. 9. Comparison of observed horizontal deformations of sections of observation line and modelled ones calculated from displacements of endpoints of line sections

Tab. 2. Maximum horizontal deformation ε_{max} [mm/m] on basis on horizontal displacements over different year ranges

1994–2000				2010–2019				1994–2019			
No.	Observed	Modelled	Difference	No.	Observed	Modelled	Difference	No.	Observed	Modelled	Difference
A21	+0.2	+1.4	+1.2	A21	–	–	–	A21	+1.0	+1.5	+0.5
A18	−2.9	−3.0	−0.1	A18	+1.3	+1.2	−0.1	A18	−2.2	−2.0	+0.2
II	+1.1	+1.9	+0.8	II	−2.2	−2.6	−0.4	II	–	–	–

Discussion

The analysis first covered the subsidence of control points on the crest of the dam. The distributions of subsidence observed over the analyzed mining operation in 1995–2010 and 2010–2019 (Fig. 4) are described well by the modelled values. This enables a more in-depth analysis of the temporal distribution of subsidence for individual points of the observation line. The distributions of the subsidence in Fig. 5 for points A15, A16, A18, and A20, confirm the correctness of the assumed values of the parameters of the calculation model. A question may be raised as to whether the observation-line points on the crest of the dam move in the same way as the measurement points on the foreland of the reservoir. For this purpose, the subsidences of points A12 and A19 were compared with those of the adjacent points at the foot of the slope of the reservoir (E12 and E19, Fig. 2). The vertical movement of these points is qualitatively and quantitatively consistent (Fig. 10). It follows that the dyke behaves in the same way as the terrain on which it is located. In the analyzed period, we are not dealing with the compaction of the material from which the dam is built because several dozen years have passed since its construction.

The presented analysis of the values of the measured and modelled subsidence of the terrain and the dyke of the flotation tailings reservoir confirms the usefulness of the Knothe model for describing the dynamic values of subsidence caused by the mining of copper ore deposits in Poland using the chamber-pillar method. At the same time, note that the subsidence caused by the exploitation did not affect the stability and functionality of the reservoir dyke. There were no significant changes in its structure, stability, and material toughness, and the dam continues to function effectively as the reservoir boundary.

The analysis of the displacement and deformation of the dyke of the flotation tailings reservoir shows that for both subsidence and horizontal deformation, the values obtained by the Knothe model are consistent with or slightly more than the measured values. It can be considered that this gives an additional safety margin, which is so important for this type of facility (Ostrowski & Ćmiel, 2008). The model correctly describes the phenomenon of rock-mass deformation and the ground surface, despite only a few parameters characterizing the rock-mass properties. However, the possibility of a phenomenon that differs from the model of displacement and deformation adopted herein should be accounted for.

During the first stage of exploitation with roof deflection in 1995–1997 (Fig. 2), increased values of displacements of the analyzed points from the northwest to the southeast were observed. On the other hand, in the second stage (operation in 2011–2014), damping of the displacement values toward the north was found (in the opposite direction to the slope of the bottom of the reservoir, the original surface area). Therefore, it can be hypothesized that the deposited sediments are moving toward the natural slope of the reservoir bottom (southern direction; see Section 2.1). This results in (i) intensified horizontal displacements in the case of mining operations to the south of the dam and (ii) limited horizontal displacements in the case of exploitations carried out north of the reservoir dyke (Fig. 11).

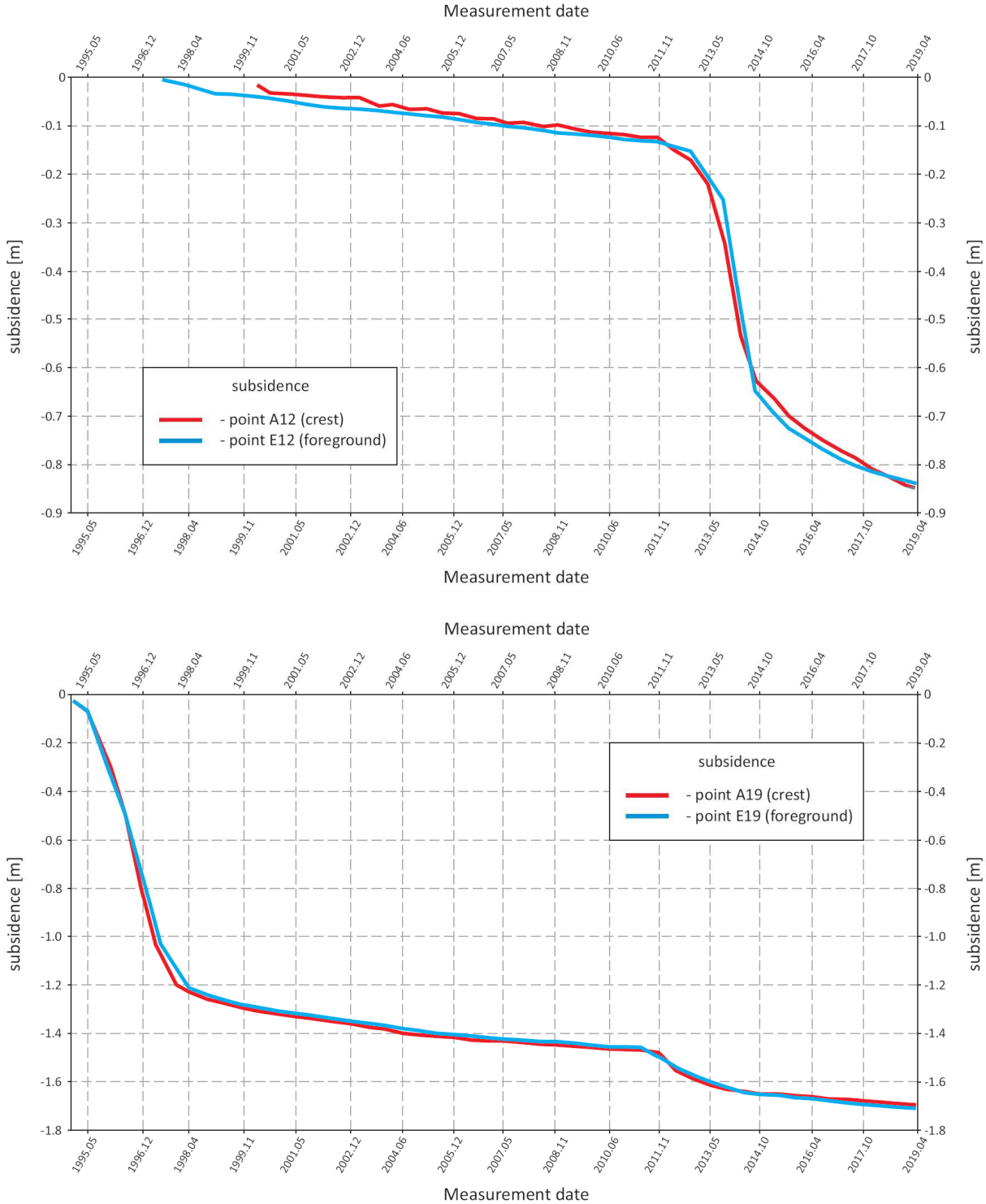

Fig. 10. Comparison of subsidence at points located on dyke (A19, A12) and the foreland of the dam (E19, E12)

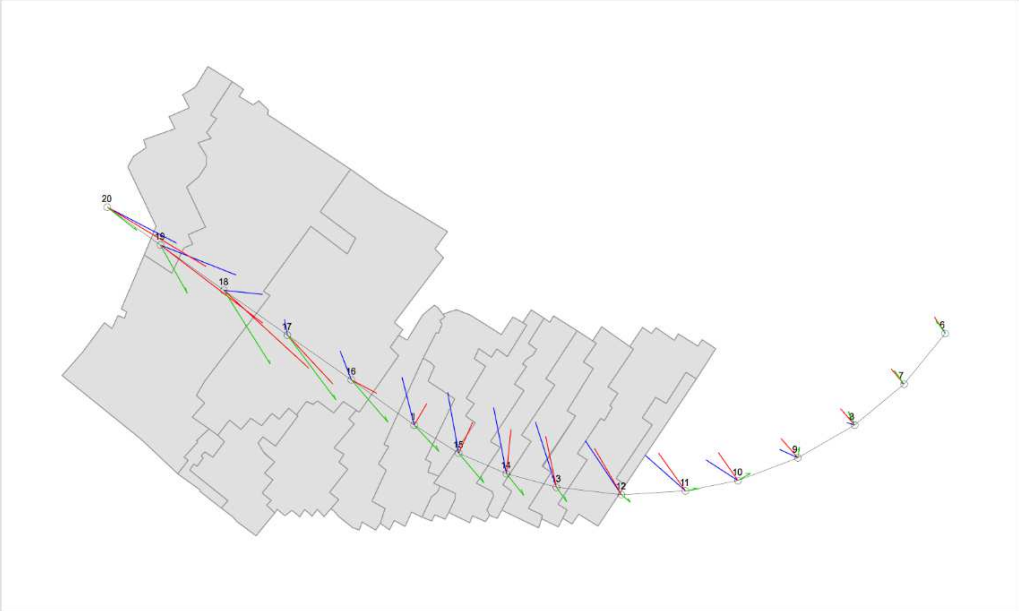

Fig. 11. Vectors of horizontal displacements of observation-line points: modelled (blue), observed (red), and difference vectors (green) indicating the intensification or damping of the movement of control points

According to the adopted theoretical model (in 1994–2000), the greatest horizontal displacement should occur over the edge of the exploitation field (i.e., at point A19). At other points, the displacements should decrease. This is shown in the graph of modelled displacements u_{max} in Fig. 7 (dashed red line). The maximum values observed are larger than the modelled ones (Eq. 4) by approximately 7 cm. At the same time, it is observed that the displacements of the points from east to west over the eastern edge of the field (point A16) decreased (attenuation occurred). It can also be concluded that the directions of the observed displacement values deviate from the modelled ones toward the south, in accordance with the slope of the natural surface of the reservoir bottom.

The same situation occurred during the subsequent operation in 2011–2014 (Fig. 2), and the observed phenomenon intensified (Fig. 7, green lines). Above the western edge of the exploitation field, the observed horizontal displacement is 73 cm, whereas the modelled displacement is only 42 cm. At the same time, over the eastern edge, the corresponding values were 27 cm (observed) versus 56 cm (modelled). This confirms the presented hypothesis on the impact of the deposited sediment masses on the displacement field caused by underground mining. This impact causes changes in the directions and values of horizontal displacements as a result of mining operations.

Figure 12 shows the observed and modelled vectors of horizontal displacements for points A12, A16, and A19 located above the edges of both operating stages. There are visible discrepancies in the directions and lengths of the vectors, resulting from the analysis presented earlier and the hypothesis put forward.

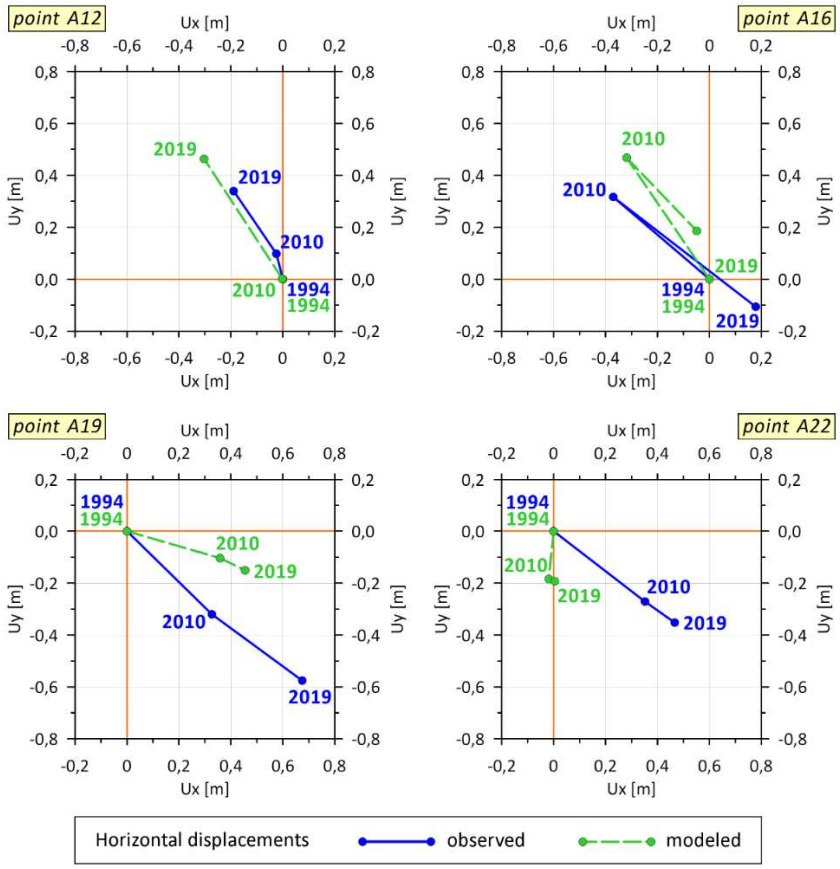

Fig. 12. Horizontal displacements of points above western (A22, A19) and eastern (A16, A12) edges of mining field

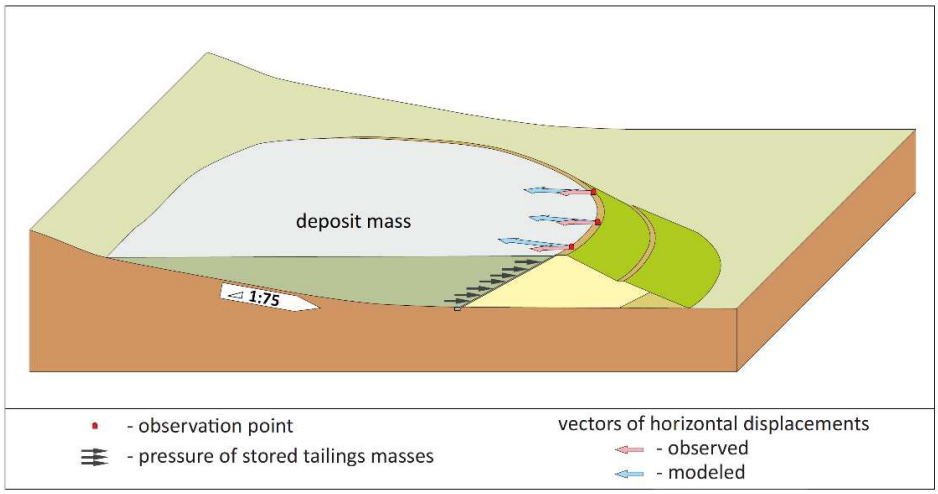

Fig. 13. Diagram of interactions and horizontal displacements of earth dam of flotation tailings reservoir

The discussed discrepancies are shown schematically in Figs. 11 and 13. The dyke movements represented by vectors can be described as follows. In the dam section between points A20 and A18, the modelled horizontal displacements directed to the centre of the exploitation field show a slight deviation in relation to the edge of the reservoir. The directions of displacements and edges of the dyke along this section are similar (Fig. 11), and the deviation of the displacements toward the inside of the reservoir is visible. The influence of the deposited sediment masses (with direction corresponding to the natural slope of the bottom surface of the reservoir), postulated in the hypothesis, leads in this case to determine the direction of the observed horizontal displacements toward the outside of the object. The movement of the sediment masses activated by the deformation process simultaneously increases the values of the observed displacements. This is due to the sediment pressure toward the southeast and not the direct impact of mining under the facility.

At points A17 and A16, there is a large difference in the directions of the modelled and observed horizontal displacements, reaching nearly 160°. The reason is the opposite direction of the modelled displacements in relation

to the direction of the pressure of the sediment masses. The resultant value of horizontal displacement at these points depends on the value of the component related to the pressure of the masses on the dam.

In the further part of the dam (from point II to the east), because of the change in the direction of the edge of the reservoir, the situation in the displacement field changes. The component of the displacement vector related to sediment pressure causes the reduction of large modelled values, deviating from the edge of the reservoir at a significant angle exceeding 40°.

The increasingly lower values of the component of the displacement vector related to the sediment pressure (Fig. 11, green vectors) shown in the northeast direction result in the increasingly lower height of the dyke (natural elevation). Therefore, the stresses generated by the pressure of sediments on the dam in this direction also decrease.

The aforementioned phenomenon may also partly result from the area's geological structure in which the reservoir is located. The ground of the object is formed by fluvioglacial sediments in the form of sands, gravels, and clays of varying thickness from 30 to 50 m, which rest on a several-dozen-meter layer of Pliocene clays, constituting the top of the Neogene. In general, the thickness of the Quaternary, Palaeogene, and Neogene formations is approximately 300 m. Below it are mottled sandstones (Triassic) and formations belonging to Zechstein (Piestrzyński, 2008). The layer of clay subjected to loading the reservoir with sediments may additionally constitute a sliding layer for the movement of the Quaternary formations overlying it.

The pressure of sediments "flowing" on the sloped bottom of the reservoir and the possible translation of the rock-mass layer on the sliding layer disturb the field of horizontal displacements, which would be the result of a direct impact of mining operations. In the case of vertical displacements (subsidence), the analysis showed a high convergence of the observed and modelled values. It can therefore be concluded that the vertical movements, in this case, are correctly described by the Knothe model.

The values of horizontal deformations, in accordance with the results presented in Table 2 and Figs. 8 and 9, obtained as a result of modelling, are partially consistent with the measured values. The values modelled in the places of maximum values are mostly higher (3–58%) than the observed values. Therefore, a certain safety margin is ensured in the case of forecasting changes in the deformation state of similar objects in the future.

However, a significant discrepancy was found in the tensile strain zone at the western border of the field exploited in 1995–1997 with the roof deflection system. The minimum value of deformations determined from the observations was only $\varepsilon_{obs} \approx +0.2$ mm/m, and the modelled value was $\varepsilon_{mod} \approx +1.4$ mm/m. This additionally confirms the hypothesis presented in the analysis of horizontal displacements. The effect of the forces related to the pressure of sediment masses on the reservoir dyke to some extent limits the displacement values, resulting in a reduction of deformations along the dyke of the reservoir described by horizontal deformations.

Further analyzing the exploitation in 2011–2014, one can notice a smaller difference in the modelled values and the observed horizontal deformations. The total deformations amounted to $\varepsilon_{obs} = +1.0$ mm/m and $\varepsilon_{mod} = +1.5$ mm/m, respectively. Increasing the size of the exploitation field in the second analyzed stage already generated an increased impact (the so-called large field) on the moving rock mass (Popiołek, 2009). This is confirmed by the values of the deformation increment in 2010–2019. In this case, the theoretical values are lower than the measured values (+0.3 and +0.9 mm/m), i.e., different from the general trend. The expansion of the exploitation field in the second stage of exploitation was an impulse for the disclosure of partially residual influences from the exploited field in the first stage. However, the total values of the measured horizontal tensile strains $\varepsilon(+)$ are generally smaller than the model values.

In summary, we can state that the exploitation in question, carried out with roof deflection in 1995–2014 to the height of the service door $m = 3.0 \div 3.8$ m, caused the maximum horizontal deformations along the dyke, determined on the basis of geodetic observations within the range from $\varepsilon_{obs} \approx -2.9$ to +1.2 mm/m. The values obtained with the Knothe model for the parameters determined in the first part herein range from $\varepsilon_{mod} \approx -2.9$ to +1.8 mm/m. The greater value of compressive strain is the result of summing up the effects inside the exploitation field from its eastern and western edges.

The maximum value of horizontal deformation $\varepsilon_{\max\_mod}$ (Eq. 15), in accordance with the model and the adopted value of parameter B (Eq. 8), can be determined on the basis of the maximum observed tilt $T_{\max\_obs}$ along the observation line:

$$\varepsilon_{max\ \_mod} = 0.48 \cdot T_{max\_obs} \tag{15}$$

The maximum value of the slope $T_{\max\ \_obs} = 2.9$ mm/m was observed on the section between points A12 and A15 over the eastern edge of the exploitation field (Fig. 4). According to Eq. (15), the deformation value in this section is $\varepsilon = +1.4$ mm/m, i.e., slightly higher than the measured value of $\varepsilon_{\mathrm{obs}} = +1.2$ mm/m. Thus, an additional conclusion follows that in the absence of measurements of changes in the length of the sides of the observation lines, it is possible to determine the probable value of the maximum horizontal deformations on the basis of the determined value of the maximum slope T_{max_obs} of the subsidence trough. As shown in the first part herein, the modelled subsidence values are consistent with the actual values, and the values of the forecast horizontal deformations will also be similar to the actual values.

The presented values of horizontal deformations correspond to categories I and II of the mining area (ε < 3.0 mm/m) (A. Malinowska & Hejmanowski, 2010). Observing the behaviour of the dyke in the period of exploitation development and the disclosure of maximum deformations, no significant changes were found in the degree of compaction of the material from which it is built and its tightness. The basic role of the dyke and the safe operation of the reservoir have not been endangered. This is another argument confirming that the problem of limiting values of deformation indexes should be reconsidered when designating protective pillars for dykes and flotation tailings reservoirs in operation and under construction. Currently, the strict limit value for these objects is adopted, i.e., ε = 0.3 mm/m, corresponding to category 0 of the mining area (A. Malinowska & Hejmanowski, 2010). Analyses were also carried out in which this value was limited to ε = 0.15 mm/m. It should be taken into account that such structures are not rigid; as earth structures, they can transfer deformations caused by mining exploitation without damage. Hence the conclusion that the limit values used in the construction of protective pillars do not have to be so strict. Of course, the conclusions drawn herein may apply to dykes of similar construction and total height not exceeding 22 m.

Conclusion

In each case of modelling or forecasting the impact of mining operations, the expert is faced with a dilemma: which model to use for calculations, and which parameter values of this model will give values closest to the actual ones? The considerations presented herein showed the complexity of the problem and the possibility of significant anomalies of the actual deformation distribution in relation to the assumptions of the adopted model. The discrepancies between the theoretical and established measurements of the deformation state can be large. Current geodetic measurements are not only used to record *a posteriori* deformations. The proper use of the results of current measurements is also a possibility for the interpreter to infer the behaviour of the rock mass and the surface or possible anomalies that must be accounted for when assessing the increments of deformation indicators resulting from subsequent stages of exploitation. For *a priori* calculations, only the ranges of parameters and coefficients characterizing the analyzed exploitation and geological conditions (rock mass) can be determined. *A priori* prognostic calculations should be performed invariants for various combinations of parameters (Gruszczyński et al., 2018; Niedojadło & Gruszczyński, 2015) characterizing the rock mass and the exploitation. This enables the accuracy (standard deviation) of the determined values of the deformation rates to be estimated.

The presented analyses and considerations show that the dynamics of revealing the impacts in the conditions of copper ore mines are greater than what was previously believed and obtained in prognostic calculations. This is confirmed by the results of measurements of the displacements of the ground surface points.

The presented considerations confirm that the problem of limiting values of deformation indexes should be reconsidered when designating protective pillars for dykes and flotation tailings currently operating and under construction. Currently, for these objects, the limit value of deformation that can be transferred by the dam crest is ε = 0.3 mm/m. This corresponds to the limit value of zero of the mining area category, which describes the minimum risk to objects within its range. The conclusions resulting from the present work show that dykes, as earth structures, may be subject to significantly greater impacts without limiting the parameters determining the safe operation of the entire flotation tailings reservoir. This was demonstrated on the example of a dyke with the structure presented herein and with a total height not exceeding 22 m. More-general conclusions can be presented on the basis of the results of research carried out on objects with a greater height of earth dams.

References

Ambrožič, T., & Turk, G. (2003). Prediction of subsidence due to underground mining by artificial neural networks. *Computers and Geosciences*, 29(5), 627–637. https://doi.org/10.1016/S0098-3004(03)00044-X

Budryk, W. (1953). Determining of the horizontal deformations values of the terrain. *Archives of Mining Steel Industry*, 1(1), 63 – 74 (in Polish).

Byrnes, R. (2003). Case Studies in the Application of Influence Functions to Visualising Surface Subsidence. In N. Aziz (Ed.), Coal Operators' Conference (pp. 90–100). University of Wollongong & the Australasian Institute of Mining and Metallurgy.

Ćwiakała, P., Gruszczyński, W., Stoch, T., Puniach, E., Mrocheń, D., Matwij, W., … Wójcik, A. (2020). UAV applications for determination of land deformations caused by underground mining. *Remote Sensing*, 12(11). https://doi.org/10.3390/rs12111733

Dawei, Z., Lizhuang, Q., Demin, Z., Baohui, Z., & Lianglin, G. (2020). Unmanned Aerial Vehicle (UAV) Photogrammetry Technology for Dynamic Mining Subsidence Monitoring and Parameter Inversion: A Case Study in China. *IEEE Access*, 8, 16372–16386. https://doi.org/10.1109/ACCESS.2020.2967410

Fathi Salmi, E., Nazem, M., & Karakus, M. (2017). Numerical analysis of a large landslide induced by coal mining subsidence. *Engineering Geology*, 217, 141–152.

https://doi.org/https://doi.org/10.1016/j.enggeo.2016.12.021

Gama, F. F., Paradella, W. R., Mura, J. C., & de Oliveira, C. G. (2019). Advanced DINSAR analysis on dam stability monitoring: A case study in the Germano mining complex (Mariana, Brazil) with SBAS and PSI techniques. *Remote Sensing Applications: Society and Environment*, 16. https://doi.org/10.1016/j.rsase.2019.100267

Grebby, S., Sowter, A., Gluyas, J., Toll, D., Gee, D., Athab, A., & Girindran, R. (2021). Advanced analysis of satellite data reveals ground deformation precursors to the Brumadinho Tailings Dam collapse. *Communications Earth & Environment,* 2(1), 1–9. https://doi.org/10.1038/s43247-020-00079-2

Gruszczyński, W. (2007). Application of neural networks for prediction of deformations modelling (Ph.D. thesis, in Polish) (AGH-UST). AGH-UST. Retrieved from https://winntbg.bg.agh.edu.pl/rozprawy/9943/full9943.pdf

Gruszczyński, W., Niedojadło, Z., & Mrocheń, D. (2018). Influence of model parameter uncertainties on forecasted subsidence. *Acta Geodynamica et Geomaterialia*, 15(3), 211–228. https://doi.org/10.13168/AGG.2018.0016

Guzy, A., & Malinowska, A. A. (2020). Assessment of the impact of the spatial extent of land subsidence and aquifer system drainage induced by underground mining. *Sustainability*, 12(19), 7871. https://doi.org/10.3390/SU12197871

Hejmanowski, R. (2004). Modelling in time and space of deformation caused by open stope mining in a layered orebody. Kraków (in Polish): Uczelniane Wydawnictwa Naukowo-Dydaktyczne AGH.

Jiang, Y., Misa, R., Tajduś, K., Sroka, A., & Jiang, Y. (2020). A new prediction model of surface subsidence with Cauchy distribution in the coal mine of thick topsoil condition. *Archives of Mining Sciences*, 65(1), 147–158. https://doi.org/10.24425/ams.2020.132712

Jiránková, E., Waclawik, P., & Nemcik, J. (2020). Assessment of models to predict surface subsidence in the Czech part of the upper silesian coal basin-case study. *Acta Geodynamica et Geomaterialia*, 17(4), 469–484. https://doi.org/10.13168/AGG.2020.0034

Jóźwik, M., Jura, J., Szymczyk, M., Mazur, J., & Tarasek, W. (2000). Surveying observations of earth dams of large floatation tailings reservoirs. Proceedings of the 11th International Congress of ISM, 503–506. Kraków, 4-8 September.

Jura, J. (1994). Deformation in the dam and the foreland of a large sedimentary reservoir affected by mining exploitation works. Proceedings of the 9th Congress ISM. Praha, 18-22 April.

Jura, J., Niedojadło, Z., & Stoch, T. (2013). Horizontal displacements in view of a priori and a posteriori modeling. XV International Society for Mine Surveying Congress, 791–804. Aachen.

Karmis, M., Agioutantis, Z., & Andrews, K. (2008). Enhancing Mine Subsidence Prediction and Control Methodologies. 27th International Conference on Ground Control in Mining, 131–136. Morgantown, West Virginia, USA, 29-31 July.

Knothe, S. (1953). Time influence on a formation of a surface subsidence. *Archives of Mining Steel Industry*, 1(1), 1–7 (in Polish).

Knothe, S. (1957). Observations of surface movements under influence of mining and their theoretical interpretation. Proceeding European Congress on Ground Movement, 210–218. Leeds.

Kowalski, A. (2007). Transient mining surface deformations in the prediction accuracy aspect. Katowice, Poland (in Polish): Central Mining Institute.

Kowalski, A. (2011). The assessment of forecasting accurafcy-in the case of mining deformations of terrain surface. Bezpieczeństwo Pracy i Ochrona Środowiska w Górnictwie, (1), 3–9 (in Polish).

Kratzsch, H. (1983). Mining Subsidence Engineering. Berlin Heidelberg New York: Springer-Verlag. https://doi.org/10.1007/978-3-642-81923-0

Kwiatek, J. (2007). Building object in mining areas. Katowice, Poland (in Polish): Central Mining Institute.

Kwinta, A. (2011). Application of the least squares method in determination of the Knothe deformation prediction theory parameters. *Archive of Mining Sciences*, 56(2), 319–329.

Kwinta, A. (2012a). Prediction of strain in a shaft caused by underground mining. *International Journal of Rock Mechanics and Mining Sciences*, 55, 28–32. https://doi.org/10.1016/j.ijrmms.2012.06.007

Kwinta, A. (2012b). Procedure of determination of Knothe theories parameters. In Kowal (Ed.), Objects protection on mining areas (pp. 171–179 (in Polish)). Central Mining Institute.

Malinowska, A. A., Witkowski, W. T., Guzy, A., & Hejmanowski, R. (2018). Mapping ground movements caused by mining-induced earthquakes applying satellite radar interferometry. *Engineering Geology*, 246(February), 402–411. https://doi.org/10.1016/j.enggeo.2018.10.013

Malinowska, A., & Hejmanowski, R. (2010). Building damage risk assessment on mining terrains in Poland with GIS application. *International Journal of Rock Mechanics and Mining Sciences*, 47(2), 238–245. https://doi.org/10.1016/j.ijrmms.2009.09.009

Malinowska, Agnieszka, Hejmanowski, R., & Dai, H. (2020). Ground movements modeling applying adjusted influence function. *International Journal of Mining Science and Technology*, 30(2), 243–249.

https://doi.org/https://doi.org/10.1016/j.ijmst.2020.01.007
Matwij, W., Gruszczyński, W., Puniach, E., & Ćwiąkała, P. (2021). Determination of underground mining-induced displacement field using multi-temporal TLS point cloud registration. *Measurement,* 180, 109482. https://doi.org/10.1016/j.measurement.2021.109482
Niedojadło, Z. (2008). Problems of exploitation of the copper deposit in shaft protection pillars in the conditions of LGOM. Kraków (in Polish): AGH-UST Publishing House.
Niedojadło, Z., & Gruszczyński, W. (2015). The impact of the estimation of the parameters values on the accuracy of predicting the impacts of mining exploitation. *Archive of Mining Sciences*, 60(1), 173–193. https://doi.org/10.1515/amsc-2015-0012
Niedojadło, Z., Sieradzy, K., & Spólnik, A. (2012). Settlement of the real state of shaft deformations in the Legnica–Głogów Copper Area (LGOM). *Przegląd Górniczy*, 68(8), 166–173 (in Polish).
Ostrowski, J. (2015). Surface deformations of protected mining area. Kraków (in Polish): Agencja Wydawniczo-Poligraficzna Art-Tekst.
Ostrowski, J., & Ćmiel, A. (2008). The use of a logit model to predict the probability of damage to building structures in mining terrains. *Archives of Mining Sciences*, 53(2), 161–182.
Owen, J. R., Kemp, D., Lèbre, Svobodova, K., & Pérez Murillo, G. (2020). Catastrophic tailings dam failures and disaster risk disclosure. *International Journal of Disaster Risk Reduction*, 42. https://doi.org/10.1016/j.ijdrr.2019.101361
Peng, S. S. (1992). Surface subsidence engineering. Society for Mining, Metallurgy, and Exploration Littleton, CO (USA).
Piestrzyński, A. (Ed.). (2008). Monografia KGHM Polska Miedź SA. Lubin (in Polish): KGHM Cuprum.
Popiołek, E. (Ed.). (1995). Verification of the parameters of the Knothe-Budryk and Kochmanski theory in the LGOM copper ore mines based on the results of geodetic observations (unpublished). Kraków (in Polish): Research studies of Departament of Mining Areas Protection AGH-UST.
Popiołek, E. (Ed.). (1996). Verification of the parameters of the Knothe-Budryk and Kochmanski theory in the LGOM copper ore mines based on the results of geodetic observations (unpublished). Kraków (in Polish): Research studies of Departament of Mining Areas Protection AGH-UST.
Popiołek, E. (2009). Protection of mining areas. Kraków (in Polish): Publishing house of AGH-UST.
Popiołek, E., & Ostrowski, J. (1978). Relationship between the slopes and horizontal displacements of the terrain in the finally formed subsidence basins. *Ochrona Terenów Górniczych*, (46), 40–45 (in Polish).
Puniach, E., Gruszczyński, W., Ćwiąkała, P., & Matwij, W. (2021). Application of UAV-based orthomosaics for determination of horizontal displacement caused by underground mining. I*SPRS Journal of Photogrammetry and Remote Sensing*, 174(December 2020), 282–303. https://doi.org/10.1016/j.isprsjprs.2021.02.006
Reddish, D. J., & Whittaker, B. N. (2012). Subsidence: Occurrence, Prediction and Control. Elsevier Science. Retrieved from https://books.google.pl/books?id=J9B-iaMoUNwC
Sopata, P., Stoch, T., Wójcik, A., & Mrocheń, D. (2020). Land surface subsidence due to mining-induced tremors in the upper silesian coal basin (Poland)—case study. *Remote Sensing*, 12(23), 1–17. https://doi.org/10.3390/rs12233923
Sroka, A., & Schober, F. (1983). Die Berechnung von Bodenbewegungen über Kavernen unter Berücksichtigung des zeitlichen Konvergenz und Gebirsverhaltens. Kahli Und Steinsaltz, 8(10 (in German)).
Stoch, T. (2019). Horizontal displacements in mining areas protection. Kraków (in Polish): AGH-UST Publishing House.
Stupar, D. I., Rošer, J., & Vulić, M. (2020). Investigation of unmanned aerial vehicles-based photogrammetry for large mine subsidence monitoring. *Minerals*, 10(2). https://doi.org/10.3390/min10020196
Tajduś, K. (2015). Analysis of horizontal displacement distribution caused by single advancing longwall panel excavation. *Journal of Rock Mechanics and Geotechnical Engineering*, 7(4), 395–403. https://doi.org/10.1016/j.jrmge.2015.03.012
Tajduś, K. (2009). New method for determining the elastic parameters of rock mass layers in the region of underground mining influence. *International Journal of Rock Mechanics and Mining Sciences*, 46(8), 1296–1305. https://doi.org/https://doi.org/10.1016/j.ijrmms.2009.04.006
Witkowski, W. T. (2014). Implementation of the least squares method in determining the parameters of Knothe's theory. *Geomatics and Environmental Engineering*, 8(3), 107–117. https://doi.org/10.7494/geom.2014.8.3.107
Witkowski, W. T. (2017). Modeling of ground surface subsidence due to hydrogeological changes with the use of artificial intelligence (Ph.D. thesis, unpublished, in Polish). AGH-UST.
Xu, N., Kulatilake, P. H. S. W., Tian, H., Wu, X., Nan, Y., & Wei, T. (2013). Surface subsidence prediction for the WUTONG mine using a 3-D finite difference method. *Computers and Geotechnics*, 48, 134–145. https://doi.org/10.1016/j.compgeo.2012.09.014
Yan, J., Lun, Y., Yue, J., Preuβe, A., & Sroka, A. (2018). The Application and Development of Knothe Influence Function in China. *Prace Instytutu Mechaniki Górnotworu PAN*, 20(2), 137–144.